EPJ Nuclear Sci. Technol. **9**, 34 (2023)

https://doi.org/10.1051/epjn/2023018

EPJ Nuclear Sciences & Technologies

Available online at:
https://www.epj-n.org

Templates of Expected Measurement Uncertainties: a CSEWG Effort, Cyrille De Saint Jean and Denise Neudecker (Guest editors)

REGULAR ARTICLE

OPEN ACCESS

Templates of expected measurement uncertainties for total neutron cross-section observables

Amanda M. Lewis[1,*], Allan D. Carlson[2], Donald L. Smith[3], Devin P. Barry[1], Robert C. Block[4], Stephen Croft[5], Yaron Danon[4], Manfred Drosg[6], Michal W. Herman[7], Denise Neudecker[7], Naohiko Otuka[8], Henrik Sjöstrand[9], and Vladimir Sobes[10]

[1] Naval Nuclear Laboratory, Schenectady, NY 12301-1072, USA
[2] National Institute of Standards and Technology, Gaithersburg, MD 20899-8463, USA
[3] Argonne National Laboratory, Argonne, IL 60439-4842, USA
[4] Rensselaer Polytechnic Institute, Troy, NY 12180, USA
[5] Lancaster University, Lancaster LA1 4YW, UK
[6] University of Vienna, 1010 Vienna, Austria
[7] Los Alamos National Laboratory, Los Alamos, NM 87545, USA
[8] International Atomic Energy Agency, 1400 Vienna, Austria
[9] Uppsala University, 75120 Uppsala, Sweden
[10] University of Tennessee, Knoxville, TN 37996, USA

Received: 3 May 2023 / Received in final form: 6 September 2023 / Accepted: 15 September 2023

Abstract. This paper provides a template of expected uncertainties and correlations for measurements of total neutron cross-section observables by transmission. Measurements with time-of-flight and mono-energetic neutron sources are covered. The information required for evaluations in the resonance region and high energy region is detailed, along with the template of uncertainties and correlations that can be used in the absence of other information.

1 Introduction

The neutron total cross-section is one of the most straightforward reactions to measure. This is the cross-section for all types of interactions between the incident neutron and the target nucleus–scattering or absorption, direct or compound. As the sum of all of the reaction cross sections for a particular isotope, precise experimental values provide important constraints in evaluations.

The total cross-section is measured by transmission, the fraction of the incident neutron beam that is transmitted through the sample. The time-of-flight (TOF) method can be employed to measure energy-dependent transmission over a range of neutron energies, or mono-energetic neutron sources can be utilized to measure transmission at discretized and well-characterized incident neutron energies. Transmission measurements can have very low uncertainties, with total experimental uncertainties around 1% regularly reported in EXFOR [1]. As the fundamental quantity of interest is a ratio, several sources of uncertainty that are significant in other reaction measurements are minimized.

This work is part of a topical issue on templates of expected measurement uncertainties. Reference [2] introduces the purpose and use of the templates. The whole series provides templates for different neutron-induced reaction observables. This work follows the same structure as the templates, starting with a high-level description of the measurements and data analysis given in Section 2. The evaluation process and what information is useful to an evaluator outlined in Section 3. Finally, the template of expected uncertainties and correlations, which can be used to estimate missing uncertainty values in the absence of specific information, is detailed in Section 4. The present work is an updated and expanded version of work originally published as part of the dissertation [3] of the first author.

2 Measurement types

For the total cross-section, the only measurement method is based on the transmission of a neutron beam through the sample. The transmission, T, is related to the total cross-section, σ_{tot} (in barns/atom), by the non-linear relation,

$$T = e^{-n\sigma_{\text{tot}}}, \tag{1}$$

where n is the areal number density of the sample (in atoms/barn). The experimental transmission is the ratio

* e-mail: amandalewis@lbl.gov

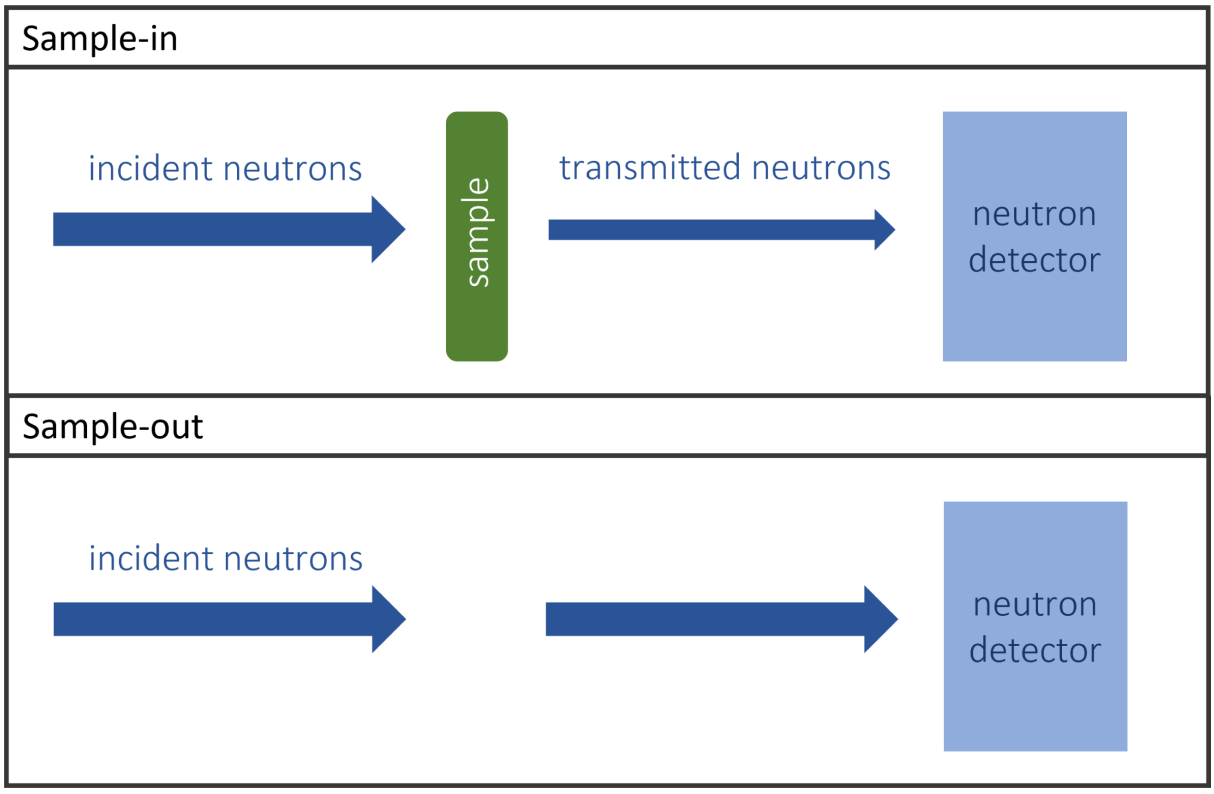

Fig. 1. Schematic drawing of the basic setup of the sample-in/sample-out transmission measurement.

of the neutrons measured with the sample in the beam to the sample out of the beam. A schematic drawing of a transmission measurement is shown in Figure 1. Both equation (1) and Figure 1 represent the fundamental definition of ideal transmission, and the application of this simple principle in real experiments is the focus of this section.

2.1 Neutron sources

TOF transmission measurements have been performed at facilities such as Rensselaer Polytechnic Institute (RPI) [4], the GEEL Electron LINear accelerator (GELINA) [5], the Oak Ridge Electron Linear Accelerator (ORELA) [6,7], the Los Alamos Neutron Science Center (LANSCE) [8], and Harwell [9]. Measurements can also be performed at reactor facilities with chopper setups (rotating shutters that create beam lines with known timing characteristics), such as at the Massachusetts Institute of Technology (MIT) [10].

Tunable mono-energetic neutron sources can be used to measure transmission at discrete neutron energies. Such sources can be created at charged particle accelerators with neutron-production reactions such as $D(d,n)^3He$ [11–14], $T(p,n)^3He$ [15,16], and $T(d,n)^4He$ [11]. Transmission measurements with mono-energetic neutron sources were most popular in the 1950s through the 1970s.

Ideally, the neutron source should be collimated into a narrow or "pencil" beam that allows for good geometry conditions, to reduce the chance that scattered neutrons will reach the detectors.

2.2 Sample characteristics

The sample diameter should be larger than the beam spot so the entire beam interacts with the sample. The sample should be as uniform as possible, with non-uniformity characterized and provided with the experimental data. The thickness can be chosen to optimize the signal-to-background ratio and counting statistics [17]. The composition of the sample should be well-characterized as it is not generally possible to separate out the reactions in different isotopes.

2.3 Detectors

The transmitted flux is measured by neutron detectors located in the beam. The neutron detector efficiency, often a significant source of uncertainty, cancels out in the ratio of the sample-in neutron counts to the sample-out neutron counts, however, the detector dead time can be significantly different and should be corrected for. Counting uncertainties fluctuate in the resolved resonance region (RRR); for transmission, they can be quite low between resonances (when cross section is low and transmission is high), and a significant source of uncertainty near the peaks of resonances. Such fluctuations are not seen in the

smoother unresolved resonance region (URR) and high energy region (HER) (also referred to as fast region) measurements.

2.4 Backgrounds

For TOF measurements, the background can generally be split into several components [18],

$$\dot{B}(t) = \dot{B}_0 + \dot{B}_\gamma(t) + \dot{B}_n(t), \tag{2}$$

with one time-independent room background rate, $\dot{B}_0$, and two time-dependent background signals, $\dot{B}_\gamma(t)$ and $\dot{B}_n(t)$. A simple schematic of these three components is shown in Figure 2. Both time-dependent components are typically fit to exponential functions. The $\dot{B}_\gamma(t)$ term represents the signal in the neutron detectors from interactions with γ rays. The $\dot{B}_n(t)$ represents the signal from neutrons that were scattered in the experimental setup or the surroundings and returned to the detector. The background can be fit using one or more "saturated resonance" or "notch" filters (resonances that are strong enough to effectively block all transmission) [19] with some corrections for the characteristics of the sample [20].

When datasets using equation (2) are reported, the background can be represented by one parameter for all of the uncorrelated uncertainty, $\dot{b}$, and one parameter for all of the correlated uncertainty, K [20],

$$\dot{B}(t) = K\dot{b}(t), \tag{3}$$

or in terms of multiple constant parameters that characterize the time-dependent background, such as in reference [21],

$$\dot{B}(t) = ae^{-bt} + \dot{B}_0, \tag{4}$$

where the a and b parameters are provided with their uncertainties.

In the case of mono-energetic neutron source measurements, the background is split into three components– in-scattering, room return, and unattenuated neutrons produced anywhere but in the gas cell or solid target [13]. In-scattering occurs when a neutron is scattered at a forward angle and still reaches the detector. For TOF measurements, the distance between the sample and the detector is typically large enough to make in-scattering negligible (assuming the beam was collimated before reaching the sample), but this is not always the case with mono-energetic neutron measurement setups, and the in-scattering contribution needs to be estimated. Corrections for in-scattering are based on the elastic scattering cross-section and angular distribution. For example, in reference [14], the correction, ΔT, on the transmission, T, due to in-scattering is given as,

$$\frac{\Delta T}{T} = \left(\frac{AR_D^2}{L^2R_s^2}\right)\frac{\sigma(0)}{\sigma_{\text{el}}}\sum_{N=1}^{\infty}\left[\left(\frac{\alpha\ell}{\lambda}\right)^N\frac{1}{N!N}\right], \tag{5}$$

where the index N represents the number of scatters the neutron underwent in the sample of cross-sectional area A and length ℓ. R_D represents the distance between the neutron source and the detector, R_s is the distance between the source and the sample, and L is the resulting distance between the sample and the detector, σ_{el} is the scattering cross-section in the sample material. Estimates were used for $\sigma(0)$, the elastic scattering cross section at 0°, α, the ratio of elastic to total cross sections (assumed to be around $\frac{1}{2}$), and λ, the mean free path of neutrons in the sample material. For the measurements in the 1950s through 1970s, there often was not sufficient experimental data to determine $\sigma(0)$ and α with high precision so theoretical expressions were used [14]. It was found that for reasonable sample sizes, the higher order terms (representing more than one scatter in the sample) contributed very little to the total in-scattering correction, which was already low–in the case of reference [14], the estimated correction was on the order of 1%. Reanalysis of the corrections with forward-modeling methods and more accurate nuclear data can improve the experimental results, but only if enough information is provided in the experimental documentation.

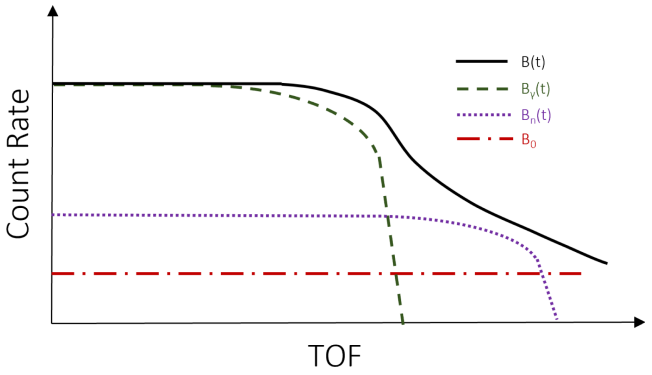

Fig. 2. Illustration of the components of the fit background, equation (2), based on reference [20]. The total time-dependent background rate, $\dot{B}(t)$, is the black solid line. It is composed of the time-independent rate, $\dot{B}_0$, (red dot-dashed line), the time-dependent γ-ray background rate in the neutron detectors, $\dot{B}_\gamma(t)$, (green dashed line), and the time-dependent background due to scattered neutrons, $\dot{B}_n(t)$, (purple dotted line). The count rate axis is on a log scale.

The room return background, β, also known as shadow background, represents neutrons produced in the gas cell or solid target that arrive at the detector without traversing the sample [13], as shown in Figure 3. The magnitude of the room return neutrons must be experimentally determined, which can be done using "shadow bars" or "shadow cones", samples thick enough to limit the transmission (or in-scattering) to very low values, similar to the saturated resonance technique in TOF measurements. For example, in reference [13], a 10-inch long nickel sample with a transmission of about 0.03% was used. The uncertainty on this transmission value due to in-scattering was assumed to be less than 50% of the value. In reference [15], a 32-cm copper shadow bar was used, with a transmission of less than 0.1%.

Finally, for mono-energetic measurements, there is a background due to neutrons that are not produced in the

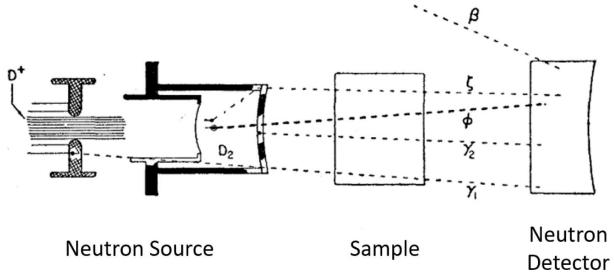

Fig. 3. Illustration of several background components for mono-energetic transmission measurements, from reference [13], which used a D(d,n)^{3}H reaction and a gas cell generator. In this diagram, ϕ represents the portion of the flux that is not attenuated by the sample and β represents the room return background. The third component of the background, neutrons produced anywhere but the gas cell or solid target, are represented by γ_1, γ_2, and ζ. In-scattering is not represented in this diagram.

gas cell or solid target, or that scatter on the walls of the neutron generator, represented by γ_1, γ_2, and ζ in Figure 3. In reference [13], it was shown that the component ζ, which scatters from the neutron generator, has a negligible impact on the measurement as long as the target walls are thin. The γ rays produced outside of the gas cell or solid target, γ_1 and γ_2, follow the same path as the primary flux but are of much lower energy and can be measured for D(d,n)^{3}He measurements by replacing the deuterium in the gas cell with ^{1}H. With this setup, there are no neutrons produced in the gas cell until deuterium builds up in the gas cell, so a measurement of this component requires repeated flushing of the H gas.

2.5 Flux normalization

As transmission is a measurement of the ratio of the sample-in and sample-out runs, the absolute flux is not needed. Beam instability and differences in the flux between the runs in a single experiment are measured with flux monitor detectors. Effects due to variations in the flux magnitude can be minimized by cycling between sample-in and sample-out runs.

For the device for indirect capture experiments on radionuclides (DICER) instrument recently developed at LANSCE to measure small samples of short-lived isotopes [22], cycling is not used due to the high precision necessary in the sample placement relative to the collimator. Instead, a rotating beam blocker and binocular collimator are used to perform sample-in and sample-out measurements simultaneously.

For mono-energetic neutron source measurements, there is little documentation of how neutron monitoring or normalization was done. In one early paper [13], the neutron flux was monitored at 90° to the beamline at the location of the neutron source. The detector counts were then normalized to the monitor counts for each run. Cycling between sample-in and sample-out runs was in some cases employed to reduce this effect [14]. In other cases, the neutron flux was measured directly using the associated particle (AP) technique of measuring the charged particle product in the neutron-production reaction. This was done in reference [12], where a D(d,n)^{3}He reaction was used.

2.6 Data analysis

The experimental observable, transmission, T_{exp}, is the ratio of the dead-time and background-corrected neutron count rates for sample-in and sample-out runs. For TOF this is calculated with

$$T_{\text{exp}} = N_T \frac{\dot{c}_{\text{in}} - \dot{B}_{\text{in}}}{\dot{c}_{\text{out}} - \dot{B}_{\text{out}}}, \tag{6}$$

where $\dot{c}_{\text{in}}$ and $\dot{c}_{\text{out}}$ are the dead-time-corrected count rates for the sample-in and sample-out runs, respectively, and $\dot{B}_{\text{in}}$ and $\dot{B}_{\text{out}}$ are the fitted background rates for each. N_T is a correction factor to account for changes between the neutron beam during the sample-in and sample-out runs. It is calculated by taking the ratio of the neutron monitors over the intervals of sample-in and sample-out measurements, m_{in} and m_{out},

$$N_T = \frac{m_{\text{out}}}{m_{\text{in}}}. \tag{7}$$

The "rates" here are not always strictly counts per second, but can be counts per second per TOF bin (which itself has a width in time) or counts per TOF bin, depending on how the normalization constant N_T is used.

For mono-energetic neutron measurements, the background corrections were sometimes applied to the transmission itself. T_0, the zeroth order (uncorrected) transmission, is first calculated,

$$T_0 = \frac{c_{\text{in}}/m_{\text{in}}}{c_{\text{out}}/m_{\text{out}}}, \tag{8}$$

where c is the detector counts, m is the neutron monitor counts (if using), and the subscripts indicate a sample-in or sample-out run [13]. The background corrections were then made by defining the uncorrected transmission, T_0, in terms of the true transmission, T, and the various background effects [13],

$$T = T_0 + (\gamma_1 + \gamma_2)(T - T_{12}) - (1 - T)\beta. \tag{9}$$

This allows for the correction of the background components γ_1 and γ_2 based on the H-gas measurement transmission T_{12}.

In the RRR the experimental transmission is directly used for the evaluation procedure, which involves forward modeling with R-Matrix Theory [23]. For the URR, the total cross-section is sometimes extracted from the experimental transmission by the experimentalist. In these regions, the energy-averaged transmission is indirectly related to the energy-averaged total cross-section,

$$\langle T \rangle = \langle e^{-n\sigma_{\text{tot}}} \rangle, \tag{10}$$

which can be approximated by a Taylor expansion,

$$\langle T \rangle \approx e^{-n\langle \sigma_{\text{tot}} \rangle} + \frac{n^2}{2} \text{var}(\sigma_{\text{tot}}) \tag{11}$$

with higher-order terms neglected [18]. The $\mathcal{O}(1)$ term represents the transmission due to the smooth average cross-section, and the $\mathcal{O}(2)$ term represents the effects due to fluctuations in the cross-section. These effects can be significant for thick samples [24], and the significance of the $\mathcal{O}(2)$ term can be estimated using simulations of resonance realizations. The impact of the fluctuations is quantified by the ratio of the averaged transmission to the transmission of the averaged cross-section, known as the self-shielding factor, F_T,

$$F_T = \frac{\langle e^{-n\sigma_{\text{tot}}} \rangle}{e^{-n\langle \sigma_{\text{tot}} \rangle}}, \tag{12}$$

which can be used to relate the measured transmission to the average cross-section for all sample sizes. This factor can be determined experimentally with multiple sample thicknesses or predicted with calculations. To calculate the self-shielding factor, resonance parameters are sampled, Doppler-broadened, and averaged to create cross-section realizations. Such calculations can be done with MCNP [25] and NJOY [26] together, or with the dedicated code SESH [27], and should be validated with measurements as was done in reference [21]. The resonance parameters are usually taken from previous evaluations and for many URR experimental datasets the self-shielding correction is performed and the dataset is reported as cross-section,

$$\langle \sigma_{\text{tot}} \rangle = -\frac{1}{n} \ln \frac{\langle T_{\text{exp}} \rangle}{F_T}. \tag{13}$$

If this correction is not performed by the experimentalist, the evaluator should calculate it before using the dataset in the evaluation. Self-shielding becomes less significant at higher energies where the cross-section fluctuations are not as strong [24], and for measurements in the high-energy region, the correction is not applied.

3 Information needed for evaluations

3.1 Evaluation methodologies

The evaluation process for the total cross-section depends on the energy region of interest. In the RRR, cross sections are represented by the parameters of individual resonances: the resonance energy, E_R, the neutron width, Γ_n, and widths for each open reaction channel. The parameters are fit using available transmission, capture yield, and fission datasets and a particular R-Matrix [23] approximation. This fitting is done by forward modeling because the experimental effects like Doppler-broadening cannot be unfolded to extract the underlying parameters [28]. Instead, resonance parameter values are used to calculate a theoretical cross section which is convolved with the experiment resolution function, $R(t_t, E_n)$, and compared to the experimental quantity. The resolution function is used to compare the cross-section to transmission by modeling the neutron source, the sample, and the detector setup to determine the distribution of neutron energies in time. In practice, most RRR evaluations are based on Bayesian updating or least-squares fitting utilizing a previous evaluation as a prior if needed. Commonly used codes include SAMMY [29], REFIT [30], and EDA [31]. In the URR, the individual resonances can no longer be experimentally resolved. Averaged parameters are fit assuming particular distributions–the Wigner distribution for resonance spacing [32], and χ^2_ν distributions for the widths [33]. A URR evaluation produces values for averaged parameters such as the scattering radius, R', the neutron strength, S_ℓ, or neutron widths, $\langle \Gamma_n^\ell \rangle$, gamma widths, $\langle \Gamma_\gamma^\ell \rangle$, and average resonance spacing, D_ℓ. In the HER, the resonances overlap creating a smooth cross-section that can be predicted by physical models like the optical model. An HER evaluation produces point-wise total cross-section values.

3.2 Reporting systems

Previous work [34] has documented the information that should be included with resonance region datasets to allow evaluators to accurately reproduce the experimental conditions. One extensively developed method for reporting uncertainties is the analysis of geel spectra (AGS) data analysis framework [35,36]. These systems allow for clear, consistent reporting of the uncertainties and sensitivities in the EXFOR [1] compilations. For RRR transmission measurements, values reported for each data point are T_{exp} and the uncertainty on T_{exp}, the partial uncertainty due to the counting statistics, the background, and the flux normalization, N_T. For URR transmission measurements, the values reported for each data point are $\langle \sigma_{\text{tot}} \rangle$, the uncertainty on $\langle \sigma_{\text{tot}} \rangle$, and the values for F_T. For both regions, the number density of the sample, n, and its uncertainty are reported for each sample used. Partial uncertainties (as the uncertainty multiplied by the sensitivity) are reported to allow the user to reconstruct the covariance matrix, as the sensitivities of many of the parameters are complicated and experiment-dependent. Other formats that separate the statistical and systematic uncertainties are used as well, for example in reference [21]. With this information, the propagation of uncertainty through the data analysis equations can be performed by an evaluator who is not familiar with all aspects of the data analysis.

The purpose of this template is to help evaluators understand the uncertainty analysis performed, update it when needed, and estimate correlation matrices when not provided [2]. Estimating unknown sensitivities is not feasible for many transmission experiments, as the signal-to-noise ratio (which determines the sensitivity values for the count and background variables) can vary by orders of magnitude between samples, facilities, and energy points. Without sensitivities provided, a user of the dataset would need to know all of the data analysis equations and

parameter values in order to propagate parameter uncertainties onto the transmission. In the absence of those (the most common case), uncertainties for parameters that are not merely multiplicative cannot be propagated onto the transmission. For example, the factor N_T is a simple multiplicative factor on T_{exp} in equation (6), so a percent uncertainty on N_T can easily be propagated to T_{exp} without knowledge of the other parameter values. The transmission has a more complicated sensitivity to other parameters, such as the sample-in background, $\dot{B}_{\text{in}}$. It would not be possible to update the transmission covariance matrix based on a new value of $\delta\dot{B}_{\text{in}}$ without sensitivity values, which highlights the importance of reporting sensitivities. For the variables that are not multiplicative factors, the templates can help the evaluator to determine whether the uncertainty analysis performed may be insufficient but cannot provide estimates of the sensitivities or the uncertainties on transmission due to the parameters.

3.3 Experiment metadata

The values of the reported quantity (transmission or total cross-section), the incident neutron energy, and the respective uncertainties are the minimum information needed for an evaluation, along with whether the presented quantity is transmission or cross-section. To fully understand, use, and assess the dataset and its uncertainties, however, more information is needed.

In many cases, information is not provided due to the difficulty of recording all of the metadata that might be useful to evaluators. In addition, little importance has been placed on publishing some of this information in journal articles, and some journals have discouraged the publication of such a large volume of information. The EXFOR database [1] or supplemental information may be a better option to store this helpful information. The IAEA Consultant's Meeting on EXFOR Data in the Resonance Region and Spectrometer's Response Functions [34] developed recommendations about the metadata that should be reported to EXFOR for RRR datasets, along with a template for doing so. One of the recommendations for experimentalists is to report the dataset as the measured observable transmission (or reaction yield), rather than derived cross-section values. Another recommendation for evaluators is to take care with older EXFOR entries, as measured transmission or yield results were sometimes divided by the areal density of the sample–giving results with the units, but not always the physical meaning, of cross-section. In these cases, the dataset may be compiled as "cross section in thin target approximation" (with, `SIG, TTA` in the reaction string) to indicate the compilation process. More information about this can be found in reference [37] and in Section 2.8 of reference [38].

For RRR datasets, evaluators should have access to the transmission, T_{exp}, and resolution function, $R(t_t, E_n)$, and for URR datasets, the transmission, T_{exp}, and the self-shielding factor, F_T, to allow for full use of the dataset.

3.3.1 Neutron sources

The resolution function, $R(t_t, E_n)$, is needed for RRR measurements to enable accurate forward modeling. Examples of how the resolution function can be documented are shown in reference [34]. Resolution functions can be presented as functional forms, code inputs, or in point-wise form. Global characterization of the resolution function of a particular facility is possible and has been done for ORELA [39], GELINA [40], and others provided in the RRR evaluation code SAMMY [29]. The resolution function is specific to particulars of an experimental setup, such as the flight path and detectors. So, values for the parameters in those global functions should be provided with each dataset.

A resolution function can be calculated for a monoenergetic source but is usually only used to validate the experimental results and is not reported with the experiment. Such information would be helpful for an evaluator to understand possible background from other reactions and should be reported if calculated.

3.3.2 Sample characteristics

The thickness, number density, composition, uniformity, and physical form of the sample can help the evaluator understand if contamination or self-shielding effects need to be modeled. It is important that the composition of the sample (natural abundance or isotopically enriched) is specified, as for transmission there is no way to distinguish between reactions in the target isotope and other isotopes in the sample. For TOF measurements in the RRR, the locations of the resonances seen in the measured transmission can help identify the contributions from the different isotopes, but the effects cannot be removed or subtracted. The composition and possible impurities of the sample are therefore essential for correctly modeling the transmission using evaluated nuclear data for the other isotopes. For transmission in the RRR, the full set of sample characteristics, including the effective sample temperature, is necessary for accurate modeling.

3.3.3 Detectors

The uncertainties on the counts for sample-in and sample-out, or combined into one uncertainty, along with the sensitivities (for TOF measurements) would allow the evaluator to update or create a covariance matrix for the dataset. The counting statistics are often the only or one of the only significant sources of fully uncorrelated uncertainty so they are important for the construction of the covariance matrix.

3.3.4 Backgrounds

The overall background uncertainty and sensitivity values should be given for each data point to allow evaluators or other users of the data to construct or update the covariance matrix for the dataset. For TOF measurements the background uncertainties can be provided as one value or split into different parameters, as in equations (3) and (4).

The initial burst of γ-rays at the start of a pulse, the "γ-flash", causes dead-time losses in the detectors,

Table 1. Uncertainty and correlation template for TOF transmission measurements for variables defined in this section. The values given are relative uncertainties in percent, on the parameter. Parameters with no recommended uncertainty values are left blank. The correlations are between different data points within the same experiment.

Uncertainty source			Unc. (%)	Corr. (i, j)
(4.1.1)	ΔE			Strong Gaussian
(4.2.1)	δn		See Table 3	Fully
(4.3.1)	$\delta \dot{c}$			Uncorrelated
(4.4.1)	$\delta \dot{b}$			Uncorrelated
(4.4.2)	δK	(saturated res.)	3	Fully
		(w/o saturated res.)	5	
(4.4.2)	$\delta \dot{B}(t)$			Strong Gaussian
(4.5.1)	δN_T	(with cycling)	1–2	Fully
		(w/o cycling)	2–6	
(4.6.1)	δF_T			Strong Gaussian

resulting in unusable data at very low TOF values. This low-TOF region (which corresponds to high incident neutron energy) can also be impacted by overlap, or "wrap-around" neutrons, which are low-energy neutrons from the preceding pulse(s). Filters can be placed in the beam to reduce these effects, such as Pb filters for the γ-flash [22,41] and Cd [22] or ^{10}B [41] for the wrap-around neutron background. Transmission or total cross-section data are typically not reported in energy regions significantly impacted by these backgrounds, so they may not be mentioned in the description of the measurement. However, discussion of any filters used and/or measurements of the wrap-around background are valuable in the assessment of the overall quality of the dataset. For example, reference [41] describes the filters and a separate run performed with a much longer pulse width, and reference [22] describes in detail how the various backgrounds in equation (2) were measured at the new DICER setup at LANSCE, and how the wrap-around neutron background was estimated.

For mono-energetic neutron sources, the uncertainties of the background corrections should be recorded. The value of the corrections themselves is not strictly needed, but having a sense of how large the corrections are allows the evaluator to understand possible biases in the dataset. The magnitude of the values $(T - T_{12})$ and β in equation (9) are especially helpful in determining the sensitivity of the measured transmission to the background components.

3.3.5 Flux normalization

The partial uncertainty on N_T, and the correction for flux differences between the sample-in and sample-out runs, should be provided for TOF measurements. As one of the fully correlated uncertainties that can vary greatly in magnitude between experiments, it is very important for correlation analysis.

3.3.6 Data analysis

For URR measurements reporting cross-section, the F_T values should be presented in addition to the uncorrected transmission values (if the sample is thick enough to require this correction). The F_T correction is not strictly an experimental correction, as it typically relies on evaluated resonance parameters for the Monte Carlo calculation. The evaluator should have access to the uncorrected transmission values to allow recalculation of F_T with updated resonance parameters as part of the evaluation process. The information about the experiment needed to perform the calculation is included in the sample information discussed above. The method for calculating F_T should be described in detail, including which code was used and what evaluated averaged values were input, along with any estimates of the uncertainty.

4 Template

If the uncertainty values detailed in the previous section are not provided with a dataset, the following template of uncertainties and correlations can be used to estimate some values. This should be undertaken only if there is no way to determine specific uncertainties of the experiment, but there is enough information about the experimental methods to make an informed estimate. The uncertainty values and correlations for TOF resonance region measurements are given in Table 1, and recommendations for mono-energetic measurements are given in Table 2. Correlations are described by a shape and a magnitude, where the shape describes the energy dependence of the

Table 2. Uncertainty and correlation template for mono-energetic transmission measurements for variables defined in this section. The values given are relative uncertainties on the parameter and are all in percent. Parameters with no recommended uncertainty values are left blank. The correlations are between different data points within the same experiment.

Uncertainty source		Unc. (%)	Corr. (i, j)
(4.1.1)	ΔE		Strong Gaussian
(4.2.1)	δn	See Table 3	Fully
(4.3.1)	δc		Uncorrelated
(4.4.3)	$\delta \Delta T$	20	Strong Gaussian
(4.4.4)	$\delta \beta$		Fully
(4.4.4)	$\delta\gamma_1$, $\delta\gamma_2$, $\delta\zeta$		Strong Gaussian
(4.5.1)	δN_T		Uncorrelated

correlation. A Gaussian shape [42],

$$\mathrm{corr}(i,j) \propto \exp\left[-\left(\frac{E_i - E_j}{\max\left(E_i, E_j\right)}\right)^2\right], \qquad (14)$$

can be used for correlations that are stronger between data points, i and j, that are closer in incident neutron energy E_i, E_j.

As discussed in more detail in Section 3.2, parameter uncertainties cannot be propagated onto the transmission or total cross-section results without sensitivities. If sensitivities are provided (as they are for the AGS system), or can be calculated (using known data analysis equations and possibly parameter values), the template values can be used to recalculate the covariance for the transmission or total cross-section. If not, these values can be used to make a qualitative assessment of the quality of the reported uncertainties.

4.1 Neutron source

4.1.1 Neutron energy (δE, ΔE)

The uncertainty on the neutron energy values or bins, δE, and on the neutron energy resolution, ΔE, are hard to estimate for TOF measurements as it depends on details of the flight path length, the timing resolution, and the method by which the calibration was performed. The neutron energy uncertainties likely have a strong Gaussian-shaped correlation between data points. The uncertainty of the neutron energy values or bins is likely to be highly correlated between experiments at the same facility, and weakly correlated between experiments at the same type of facility. For experiments performed at different types of facilities or where characterization methods are different, the uncertainties can be assumed to be uncorrelated.

For mono-energetic neutron sources, the energy uncertainty and resolution are dependent on the neutron-production reaction and the geometry of the neutron production target or cell, so an estimate should be based on this information. This uncertainty can reasonably be neglected if the cross-section is relatively constant over the energies measured. The energy uncertainty will be strongly correlated between different energy points and between experiments using the same source reaction.

4.1.2 Resolution function ($\delta R(t_t, E_n)$)

The uncertainty on the resolution function, $\delta R(t_t, E_n)$, is not a component of the uncertainty on the experimental transmission, but is needed for proper modeling of RRR transmission datasets. The values and uncertainties of the parameters used to model the resolution function in RRR evaluation codes are often not easy to extract from the presented experimental information, and their values are hard to estimate generally. The resolution function uncertainty will be highly correlated for experiments at the same facility. In these cases, the resolution function may be very similar and based on the same methods of determination. If it is known that the neutron production target was different between the two experiments, a weak correlation can be assumed due to similar characterization methods. Some correlation will also be introduced by the use of the same simulation code (from the underlying data and the geometric modeling). Further study on the uncertainties in the resolution function needs to be undertaken before recommendations can be made for experiments at different facilities.

4.2 Sample characteristics

4.2.1 Number density (δn)

The uncertainty on the number density of the sample, δn, can be estimated based on the physical form of the sample. The values are presented in Table 3. Metal samples tend to have lower uncertainties, between 0.1% and 1%, than powder samples, between 2% and 5%. The uncertainty on liquid samples depends on whether the sample is naturally liquid or is a solid sample that was dissolved into liquid

Table 3. Uncertainty template for sample number density. The values are relative uncertainties, in percent, on the number density.

Sample type	δn (%)
Metal	0.1–1
Powder	2–5
Liquid	0.1–1
Diluted liquid	2–5

for the purposes of dilution. The number density of liquid samples can be characterized to a high precision, similar to or even higher than metal samples of comparable optical thickness. Solid samples with saturated resonances are therefore sometimes dissolved into liquid in order to lower the effective n. For example, a measurement of Hf resonance parameters at RPI [43] used liquid samples, allowing for Hf number density values that could not easily be achieved with high-quality metal foils. For this typical use case, where the solvent may make up a significant portion of the sample volume, an uncertainty between 2% and 5% is more reasonable, and an analysis of the effect of the solvent and container should be undertaken. In the case of the Hf measurement at RPI, deuterated nitric acid was chosen as the solvent because it has a low cross section that is flat in the energy region measured. The effect can be measured and subtracted out using a blank sample that contains only the solvent, which is especially important for samples dissolved in moderating solvents like water. A very thin metal sample fabricated to have the same number density is likely to have an even higher number density uncertainty, so a well-characterized liquid sample (far from the solubility limit) may be the best choice for some experiments. The number density of the sample will be fully correlated between experiments using the same sample, and have a medium to high correlation for experiments using the same method/equipment for determining n. For experiments with different types of samples and different methods of measuring n, this uncertainty is uncorrelated.

4.2.2 Sample composition

No uncertainty is given for the sample composition, as it depends on the type of sample (natural abundance or isotopically enriched) and the method of production. It is important to account for contaminants in the assessment of the experiment, as reactions due to different isotopes cannot be distinguished in a transmission measurement. Additional caution must be taken with powder samples, which can have an unknown amount of moisture. The hydrogen in the absorbed water can have a large impact on the transmission and a correction must be made for this effect. The uncertainty due to well-characterized contaminants can be negligible, such as for RRR measurements where the transmission of the sample is modeled accounting for the composition. In other cases, it can be quite large, if the contaminants are not well known or if their total cross sections have large uncertainties.

4.2.3 Effective temperature

The effective sample temperature, which is needed for Doppler broadening, may have negligible uncertainty. However, with liquid samples, it is not obvious how to calculate the effective temperature and the uncertainty on this quantity should not be neglected. No recommended value is given here because it may be negligible in many experiments.

4.3 Detectors

4.3.1 Counting statistics (δc, $\delta\dot{c}$)

The uncertainty on the counts, δc, or count rate, $\delta\dot{c}$, should be provided for each data point, either separately for sample-in and sample-out runs or combined into a single variable. Estimating this uncertainty is not recommended as it is dependent on many factors that are not likely to be documented for an experiment that did not report counting statistics, such as the irradiation time, the neutron detector efficiency, and the neutron source strength. Counting statistics are uncorrelated between data points and between experiments.

4.4 Backgrounds

4.4.1 Counting statistics ($\delta\dot{b}$)

Background counting statistics may be presented as $\dot{b}(t)$ in equation (3), as part of the constants describing the background in equation (4), or at times incorporated into the overall counting statistics, $\delta\dot{c}$. Estimating this uncertainty is not recommended for the reasons given in Section 4.3.1.

The rotating beam block in the new DICER setup at LANSCE provides the unique ability to measure the scattered neutron contribution, $\dot{B}_n(t)$ in equation (2), over the entire TOF region, and subtract out the measured background [22]. Without any fitted background functions, it is likely that the background uncertainty is limited to the counting statistics, $\delta\dot{b}$, for these measurements.

4.4.2 TOF backgrounds (δK, $\delta\dot{B}(t)$)

For TOF measurements, the uncertainty on the transmission due to the background spectrum depends on the fitting methods used. With a fixed saturated resonance, it is reasonable to have uncertainties down to 3% on K, but a larger estimate of 5% may be warranted if no mention of a saturated resonance is made. It is more difficult to estimate the uncertainty on a background function as a whole, $\delta\dot{B}(t)$. The background measurement with the DICER instrument [22] shows that the smooth exponential forms are not adequate to model the background for these datasets. Further work is needed to determine if this is the case only for the unique DICER setup, or for other facilities as well. The background uncertainty provided

with the dataset can be increased if a non-exponential background is suspected in a dataset that used fitted exponential forms, but it is not immediately clear how the time dependence seen with DICER should be extrapolated to other measurements. The uncertainty δK is fully correlated between different neutron-energy data points. If the background is not represented by the fully correlated K parameter, but rather is measured or calculated (or some combination of both), the correlation is likely to be strong but not necessarily fully correlated. The uncertainty in the background for TOF measurements will be correlated between experiments using the same method and functional forms. Since many TOF experiments use the same functional form, equation (2), it is likely that this uncertainty is at least weakly correlated between TOF experiments. Stronger correlations can be assumed for experiments using the same saturated resonances.

4.4.3 In-scattering correlation ($\delta\Delta T$)

For mono-energetic measurements, the reported uncertainties on in-scattering corrections fall around 20% [11,13], but lead to small (1−2%) uncertainties on the cross-section as the corrections are usually minimal. The corrections performed in the years that this method was popular, between the 1950s and 1970s, were typically simple and were based on contemporary nuclear data. The in-scattering correction uncertainty has a strong correlation across neutron energies because the same models were used to calculate the correction at each energy. Between measurements using the same nuclear data, the in-scattering correction uncertainties will be highly correlated.

4.4.4 Neutron attenuation backgrounds ($\delta\beta, \delta\gamma_1, \delta\gamma_2, \delta\zeta$)

The uncertainties on the corrections for room return background, $\delta\beta$, and the background from neutrons not produced in the gas cell or solid target, $\delta\gamma_1, \delta\gamma_2, \delta\zeta$, were not well documented. In most cases, it was stressed that the corrections themselves were very small (<1%). For this reason, these uncertainties can be considered negligible and are not included in the template.

If $\delta\beta$ is given, it will likely be fully correlated between neutron energy points, while the other sources can be assumed to have a Gaussian-shaped correlation, as the energy of the incident deuteron (or other charged particle) affects this background.

These backgrounds will be highly correlated if the geometry and materials in the neutron source and/or facility are similar.

4.5 Flux normalization

4.5.1 Flux normalization (δN_T)

The uncertainty on the normalization, δN_T, (also referred to as monitor measurements) can be one of the more widely varying uncertainties between transmission experiments. The uncertainty on how well the monitors track the changes in the neutron beam can be estimated by the correlation between the detector and monitor count rates between runs. If cycling was used and a strong correlation was found, it can be reasonable to have uncertainties below 1%, as this uncertainty can be reduced with multiple runs. If no uncertainty was given but it is indicated that cycling was performed, an uncertainty estimate of 1% is recommended. If cycling was not performed or there is no mention of it, the uncertainty estimate should be much larger, around 3%. The uncertainty is fully correlated between data points.

For mono-energetic neutron source measurements, the flux normalization process was often not documented. There were several methods employed, including measuring the neutrons at a different angle or using the associated particle method. These methods have different uncertainties that are well-documented in other templates, such as the capture and charged-particle production template [44] and the (n, xn) template [45]. If it is given it will typically be uncorrelated between neutron energies, as usually only statistical uncertainty remains.

All flux normalization uncertainties should be independent of each other for different experiments, even those at the same facility, as it is related to random fluctuations in the neutron beam.

4.6 Data analysis

4.6.1 Self-shielding correction (δF_T)

The uncertainty on the correction for self-shielding due to cross-section fluctuations in the URR, δF_T, is not often given. These values are entirely simulated and rely on resonance parameters taken from contemporary evaluations. The magnitude of the uncertainty will depend on the nucleus, and a reasonable estimate should be made based on the state of the nuclear data used in the correction. If the correction was made as a function of incident neutron energy, the uncertainty on F_T is likely to have a strong Gaussian correlation between energies. Between datasets, a strong correlation could be expected if the same nuclear data were used for the simulations, and a weak correlation may be warranted when the same method/code was used.

5 Conclusions

This work presents a template of expected measurement uncertainties for total cross-section observables measured by transmission. The sources of uncertainty expected for time-of-flight and mono-energetic measurements are detailed, along with the methods and information needed for total cross-section evaluations in the resolved resonance region, unresolved resonance region, and high energy region. A template of measurement uncertainties and correlations is provided to allow for realistic and consistent estimated uncertainties when they are not provided with the datasets. Some sources of uncertainty cannot generally be estimated after the fact, such as the counting statistics and the neutron energy resolution. Others, such as the uncertainty on the resolution function,

$\delta R(t_t, E_n)$, are complex, and general estimates cannot be recommended until more research is done on this uncertainty.

Conflict of interests

The authors declare that they have no competing interests to report.

Funding

Work at LANL was carried out under the auspices of the National Nuclear Security Administration (NNSA) of the US Department of Energy (DOE) under contract 89233218CNA000001. We gratefully acknowledge partial support of the Advanced Simulation and Computing program at LANL funded and managed by NNSA for the DOE. S.C. warmly acknowledges support from Lancaster University.

Data availability statement

The data that were created associated with this manuscript are all within its main text and tables.

Author contribution statement

Amanda M. Lewis: writing – original draft. A.D. Carlson: writing – original draft. D.L. Smith: writing – original draft. D.P. Barry: writing – review and editing. R.C. Block: writing – review and editing. S. Croft: writing – review and editing. Y. Danon: writing – review and editing. M. Drosg: writing – review and editing. M.W. Herman: writing – review and editing. D. Neudecker: writing – review and editing. N. Otuka: writing – review and editing. H. Sjöstrand: writing – review and editing. V. Sobes: writing – review and editing.

References

1. N. Otuka et al., Towards a more complete and accurate experimental nuclear reaction data library (EXFOR): International collaboration between nuclear reaction data centres (NRDC), Nucl. Data Sheets **120**, 272 (2014)
2. D. Neudecker et al., Templates of expected measurement uncertainties, EPJ Nuclear Sci. Technol. **9**, 35 (2023)
3. A.M. Lewis, Ph.D. thesis, University of California, Berkeley, 2020
4. R.E. Slovacek et al., ^{238}U(n,f) measurements below 100 keV, Nucl. Sci. Eng. **62**, 455 (1977)
5. W. Mondelaers et al., GELINA, a neutron time-of-flight facility for high-resolution neutron data measurements, Res. Infrastruct. **11**, 19 (2006)
6. K. Guber et al., New neutron cross-section measurements at ORELA and their application in nuclear criticality calculations, Nucl. Instrum. Meth. B **241**, 218 (2005)
7. H. Beer et al., ^{178,179,180}Hf and ^{180}Ta(n,γ) cross sections and their contribution to stellar nucleosynthesis, Phys. Rev. C **26**, 1404 (1982)
8. P.W. Lisowski et al., Los Alamos National Laboratory spallation neutron sources, Nucl. Sci. Eng. **106**, 208 (1990)
9. J.E. Lynn, Helios: The new Harwell electron linear accelerator, and its scientific programme, Contemp. Phys. **21**, 483 (1980)
10. K. Sun et al., Validation of a fuel management code MCODE-FM against fission product poisoning and flux wire measurements of the MIT reactor, Prog. Nucl. Energy **75**, 42 (2014)
11. A.D. Carlson et al., Fluctuations in neutron total cross sections, Phys. Rev. **158**, 1142 (1967)
12. R. Policroniades et al., An associated particle time-of-flight facility for neutron cross section measurement, Nucl. Instrum. Meth. A **346**, 230 (1994)
13. E.M. Hafner et al., The total n-p scattering cross section at 4.75 Mev, Phys. Rev. **89**, 204 (1953)
14. A. Bratenahl et al., Neutron total cross sections in the 7- to 14-Mev region, Phys. Rev. **110**, 927 (1958)
15. D.B. Fossan et al., Neutron total cross sections of Be, B^{10}, B, C, and O, Phys. Rev. **123**, 209 (1961)
16. G.D. Kim et al., Production of monoenergetic MeV-range neutrons by ^{3}H(p,n)^{3}He reaction, J. Radioanal. Nucl. Chem. **271**, 541 (2007)
17. Y. Danon et al., Minimizing the statistical error of resonance parameters and cross-sections derived from transmission measurements, Nucl. Instrum. Meth. A **485**, 585 (2002)
18. P. Schillebeeckx, Transmission TOF measurement uncertainty components and reporting of data, in *Mini-CSEWG on Templates of Measurement Uncertainties*, CSEWG, Los Alamos, NM, April 30 – May 1 2019 (2019)
19. D.B. Syme et al., Background and resolution functions in neutron time-of-flight spectrometers, in *Proceedings of the International Conference on Nuclear Data for Science and Technology*, Antwerp, Belgium, September 6–10 1982 (1983), p. 886
20. P. Schillebeeckx et al., Determination of Resonance parameters and their covariances from neutron induced reaction cross section data, Nucl. Data Sheets **113**, 3054 (2012)
21. J.M. Brown et al., Validation of unresolved neutron resonance parameters using a thick-sample transmission measurement, Nucl. Sci. Eng. **194**, 221 (2020)
22. A. Stamatopoulos et al., New capability for neutron transmission measurements at LANSCE: The DICER instrument, Nucl. Instrum. Meth. A **1025**, 166166 (2022)
23. A.M. Lane et al., R-matrix theory of nuclear reactions, Rev. Mod. Phys. **30**, 257 (1958)
24. F.H. Froehner, Evaluation and Analysis of Nuclear Resonance Data, Tech. Rep., JEFF Report 18 (2000)
25. C.J. Werner et al., MCNP Users Manual – Code Version 6.2, Tech. Rep., LA-UR-17-29981 (2017)
26. R.E. MacFarlane et al., Methods for processing ENDF/B-VII with NJOY, Nucl. Data Sheets **111**, 2739 (2010)
27. F.H. Froehner, SESH: A Fortran IV Code for Calculating the Self-shielding and Multiple Scattering Effects for Neutron Cross Section Data Interpretation in the Unresolved Resonance Region, Tech. Rep., GA-8380 (1968)
28. V. Sobes et al., NE 697: Nuclear Data, Spring 2018, University of Tennessee, Knoxville, University Lecture, https://www.youtube.com/playlist?list=PLA-IQaSyWKTD9mMu89i3a55RrWD-8hDGQ
29. N.M. Larson, Updated Users Guide for SAMMY: Multilevel R-Matrix Fits to Neutron Data Using Bayes' Equations, Tech. Rep., ORNL/TM-9179/R8 (2008)
30. M.C. Moxon et al., GEEL REFIT, A Least Squares Fitting Program for Resonance Analysis of Neutron Transmission and Capture Data Computer Code, Tech. Rep., AEA-InTec-0630 (1991)

31. G.M. Hale, Use of R-matrix methods for light element evaluations, in *Proceedings of the Conference on Nuclear Data Evaluation Methods and Procedures* (Brookhaven National Laboratory, Upton, NY, March 1981), p. 509
32. E.P. Wigner, Random matrices in physics, SIAM Rev. **9**, 1 (1967)
33. C.E. Porter et al., Fluctuations of nuclear reaction widths, Phys. Rev. **104**, 483 (1956)
34. F. Gunsing et al., EXFOR Data in Resonance Region and Spectrometer Response Function, Tech. Rep., INDC(NDS)-0647 (2013)
35. B. Becker et al., Analysis of Geel Spectra – AGS, Tech. Rep., NEA/DB/DOC(2014)4 (2014)
36. B. Becker et al., Data reduction and uncertainty propagation of time-of-flight spectra with AGS, J. Inst. **7**, P11002 (2012)
37. N. Otsuka, Reaction yield divided by areal density, in *NRDC 2017* (International Atomic Energy Agency, Vienna, Austria, 2017)
38. N. Otuka, O. Cabellos, *Summary Report of the Technical Meeting on the International Network of Nuclear Reaction Data Centres, INDC(NDS)-0736* (International Atomic Energy Agency, Vienna, Austria, 2017)
39. C. Coceva et al., Calculation of the ORELA neutron moderator spectrum and resolution function, Nucl. Instrum. Meth. **211**, 459 (1983)
40. D. Ene et al., Global characterisation of the GELINA facility for high-resolution neutron time-of-flight measurements by Monte Carlo simulations, Nucl. Instrum. Meth. A **618**, 54 (2010)
41. P.E. Koehler, Improved ^{95}Mo neutron resonance parameters and astrophysical reaction rates, Phys. Rev. C **105**, 054306 (2022)
42. D. Neudecker et al., Template for estimating uncertainties of measured neutron-induced fission cross-sections, EPJ Nuclear Sci. Technol. **4**, 21 (2018)
43. M.J. Trbovich et al., Hafnium resonance parameter analysis using neutron capture and transmission experiments, Nucl. Sci. Eng. **161**, 303 (2009)
44. A.M. Lewis et al., Templates of expected measurement uncertainties for capture and charged-particle production cross section observables, EPJ Nuclear Sci. Technol. **9**, 33 (2023)
45. J.R. Vanhoy et al., Templates of expected measurement uncertainties for (n,xn) cross sections, EPJ Nuclear Sci. Technol. **9**, 31 (2023)

Cite this article as: Amanda M. Lewis, Allan D. Carlson, Donald L. Smith, Devin P. Barry, Robert C. Block, Stephen Croft, Yaron Danon, Manfred Drosg, Michal W. Herman, Denise Neudecker, Naohiko Otuka, Henrik Sjostrand, and Vladimir Sobes. Templates of expected measurement uncertainties for total neutron cross section observables, EPJ Nuclear Sci. Technol. **9**, 34 (2023)